

## Resistivity due to Domain Walls in Co Zigzag Wires

T. Taniyama,<sup>1</sup> I. Nakatani,<sup>2</sup> T. Namikawa,<sup>1</sup> and Y. Yamazaki<sup>1</sup>

<sup>1</sup>*Department of Innovative and Engineered Materials, Tokyo Institute of Technology, Yokohama 226-8502, Japan*

<sup>2</sup>*National Research Institute for Metals, Tsukuba 305-0047, Japan*

(Received 17 September 1998)

We report a clear manifestation of the negative magnetoresistance due to the domain wall of Co submicron zigzag wires in which the domain structures are artificially controllable by changing the orientation of the magnetic fields. The resistivity in the remanent state discontinuously drops when the domain configuration switches from the single domain to the multidomain. We attribute this to the domain wall, and deduce the decrease in the resistivity of  $-1.8 \times 10^{-6} \Omega \text{ cm}$  assuming the wall thickness of 15 nm. The origin of the negative resistive contribution due to the domain wall is also discussed compared with the existing theories. [S0031-9007(99)08782-7]

PACS numbers: 73.61.-r, 75.60.Ch, 75.70.Pa

Local spin modulation in the domain wall (DW) brings about an additional correction to the electrical resistance. In particular, this correction is significant in the mesoscopic systems such as magnetic thin films and submicron wires because of a prospective high density of DWs. Thus in recent years, research on the magnetoresistance (MR) of the ferromagnetic wires intensely addresses the DW resistivity for fundamental understanding of this phenomenon and further miniaturization of magnetic devices [1–6].

The electrical resistivity due to the DW was first reported in ferromagnetic Ni and Fe wires [1,2]. The resistivity discontinuously drops with the nucleation of the DW and rapidly reverts with the traverse of the DW through the wire. This implies that the DW contributes to the negative MR. In another approach, the negative MR was also detected in the epitaxially grown Fe wires with striped domain structures [3]. The negative MR effect has been treated theoretically within the linear response theory, where the decoherence of weakly localized electrons plays an important role [5]. Opposed to this situation, another recent experiment reported on the DW scattering that gives a positive contribution to the resistance in epitaxial Co thin films [4]. The positive MR can be also theoretically explained in terms of the admixture of spin states due to the spin flip scattering in the DW [6]. Thus, the DW contribution to the electrical resistivity is still elusive, and another approach to detect the DW resistivity is required.

In this Letter, we report a novel approach to systematically explore the DW resistivity using a Co zigzag wire. Figure 1 depicts two different domain structures in remanence induced by the field in plane but either parallel or perpendicular to the zigzag wave vector  $\mathbf{k}$ . The domain structure in Fig. 1(a) should be realized after a magnetic field is applied along  $\mathbf{k}$  owing to the shape induced anisotropy. We identify the domain structure with a single domain since the current remains parallel to the magnetization throughout the current path. On the other hand, another domain configuration shown in Fig. 1(b) is most likely after saturation perpendicular to  $\mathbf{k}$ .

The orientation of the current changes by an angle of  $180^\circ$  with respect to the magnetization passing through every corner, resulting in the fact that the current conversely senses a  $180^\circ$  DW at the corner. Thus, a comparison between the resistivities in both configurations allows us to estimate the DW resistivity. We indeed present the intrinsic contribution due to the DW to the resistivity.

The submicron zigzag Co wires used in this study were fabricated by an electron-beam lithography and lift-off technique. Resist films of  $0.4 \mu\text{m}$  were coated on undoped Si(100) substrates, and zigzag patterns were defined by exposing the electron beam accelerated with 30 kV. Cobalt film layers with a thickness of 30 nm were deposited on the patterned resist at room temperature by controlling the film thickness using a quartz crystal deposition controller. The desired geometry of the Co

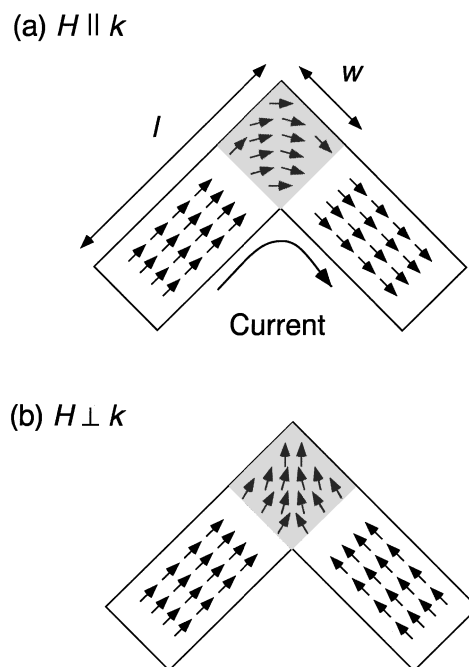


FIG. 1. Schematic illustration of the remanent domain structure near the corner.

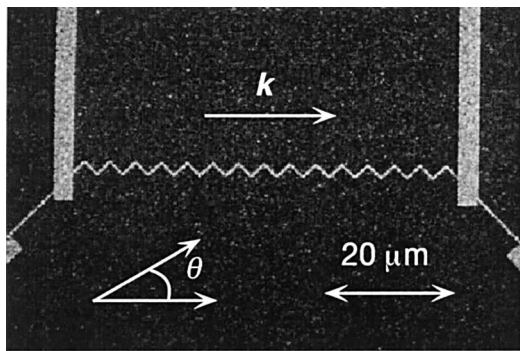


FIG. 2. SEM image of the Co zigzag wire. The zigzag wire consists of 30 straight segments, and the length between the neighboring corners is  $2.9 \mu\text{m}$  and the linewidth is  $0.25 \mu\text{m}$ .

wire was produced after the lift-off process. A scanning electron microscopy (SEM) image is shown in Fig. 2. An x-ray diffraction pattern indicates randomly oriented hexagonal polycrystalline. Magnetoresistance measurements were performed by means of a four-point ac method (10 Hz) in fields applied in the plane of the wire and at different in-plane orientations at temperatures from 5 to 200 K. A sample rotation capability enables all *in situ* measurements for one sample, which eliminates ambiguity caused by changing the probe contacts. Note that the bent angle of  $90^\circ$  at all corners effectively suppresses the difference of the anisotropic magnetoresistance (AMR) between the two configurations at the field orientation  $\theta = 0^\circ$  and  $90^\circ$  except for the corners.

First, we show the field dependent resistivities at 5 K as a function of the field orientation  $\theta$  (Fig. 3). All the field cycles were performed after applying the magnetic field of 10 kOe to diminish the magnetic history. For

the field orientation  $\theta = 0^\circ$ , the resistivity increases monotonically with decreasing fields and reaches the maximum at point *B*. The resistivity decreases more rapidly by varying the field from positive to negative values and shows an abrupt jump at point *C* ( $H = -600$  Oe). After reaching point *D*, the resistivity goes back to point *E* (*B*), and shows an alternative jump at the symmetrical point *F* ( $H_C = 600$  Oe). This MR profile is interpreted on the basis of the AMR which depends on the angle  $\alpha$  between the current and the magnetization in the following manner:  $\rho = \rho_\perp + (\rho_\parallel - \rho_\perp) \cos^2 \alpha$ , where  $\rho_\perp$  and  $\rho_\parallel$  are the resistivities when  $\alpha = 90^\circ$  and  $\alpha = 0^\circ$ , respectively [7]. When the magnetic field decreases from the positive saturation, the magnetization starts to rotate toward the nearest wire axis due to the shape anisotropy. The magnetization aligns parallel to the wire axis at point *B*, resulting in the maximum resistivity. After the field is switched into negative, the magnetization gradually deviates away from the easy axis of the shape anisotropy and reaches an unstable magnetic configuration (point *C*). The magnetization of all the segments switches simultaneously at point *C* toward the more stable alternative uniaxial direction, leading the abrupt jump of the resistivity. No change is observed in the MR profile for the field orientation up to  $30^\circ$ , besides the increase in the jump field due to the reduction of the effective field component parallel to the wire axis.

The MR profile drastically changes for  $\theta = 40^\circ$ . The domain structure at point *B* is likely as in Fig. 1(a). Reversing the magnetic field, only the magnetization of 15 segments that make an angle of  $5^\circ$  with the field switches in  $H = -800$  Oe, resulting in the slight decrease in the resistivity. By contrast, the magnetization of another 15 segments exhibits no switching even at

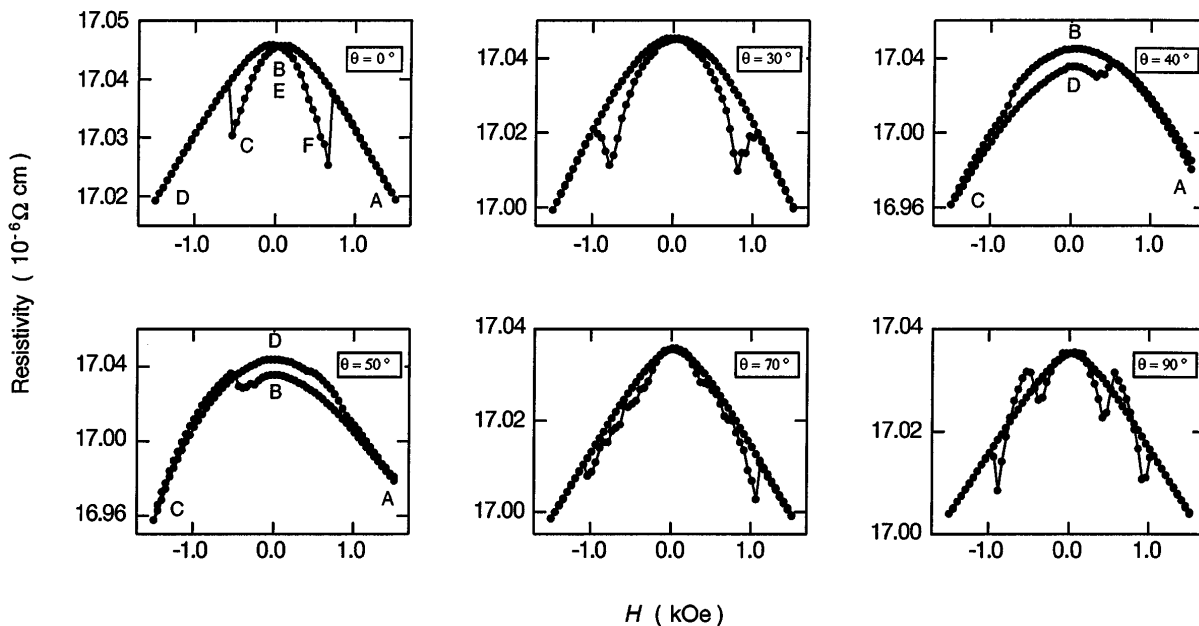


FIG. 3. Field dependent resistivities at various field orientations recorded at 5 K.

point *C*, since the field component parallel to the wire axis is quite small. The domain structure shown in Fig. 1(b) is realized by decreasing the field from point *C*. The magnetization reversed at point *B* switches again to become the single domain in  $H = 400$  Oe accompanied with the jump of the resistivity. This magnetization process occurs when the field components parallel to the wire axes are quite different between the alternate segments, which is established at about  $\theta = 45^\circ$ . A similar consideration completely accounts for the MR profile for  $\theta = 50^\circ$ , although the domain configuration at point *B* is the multidomain as in Fig. 1(b).

For  $\theta = 90^\circ$ , two clear dips appear in  $H = 400$  and  $900$  Oe, reflecting the sequential switching process of the magnetization. The domain configuration shown in Fig. 1(b) is formed in remanence in contrast to the case for  $\theta = 0^\circ$ . When the field is reversed, the magnetization favors switching so as to become the single domain structure [Fig. 1(a)] in  $H = -400$  Oe to decrease the DW energy at the corners. Further, the magnetization of another 15 segments reluctantly switches in  $H = -900$  Oe based on the magnetostatic energetics.

In order to further confirm our picture of the magnetization process, we performed the following refined measurements. First, we established the multidomain configuration shown in Fig. 1(b) by applying a field of  $10$  kOe at the orientation  $\theta = 90^\circ$ . In  $H = 0$ , hence the sample was rotated from  $\theta = 90^\circ$  to  $0^\circ$ . In this configuration the MR curve was recorded with increasing field from  $H = 0$  to  $1.5$  kOe. This enables one to determine the switching field of only the alternate 15 segments whose magnetizations make an angle of  $135^\circ$  with the field, i.e., this magnetization process corresponds to the switching from the multidomain to the single domain. The switching field of another 15 alternate segments can be also determined by applying negative fields. The MR curves are plotted in Fig. 4. The switching fields obviously coincide

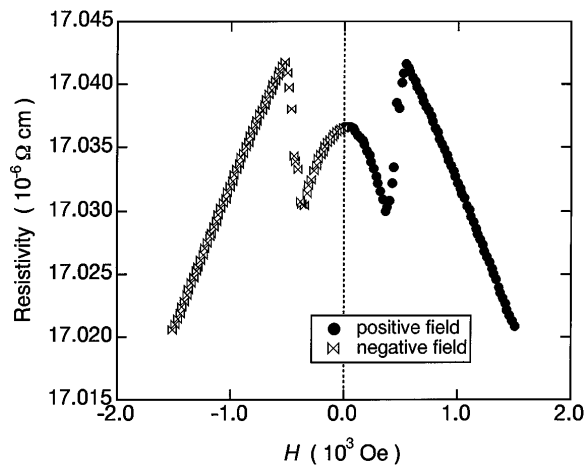


FIG. 4. Field dependent resistivities due to the switching process from the multidomain to the single domain configurations.

with the dip field of  $400$  Oe in Fig. 3, which strongly corroborates the magnetization process described above. The completely symmetrical MR profiles with respect to the field orientation guarantee the equivalence of the shape anisotropy over the entire wire.

One may claim the existence of a large out-of-plane magnetization component as observed elsewhere [4]. However, the resistance of the present sample exhibits no saturation in the field perpendicular to the plane even in  $H = 15$  kOe, although the resistance in the in-plane field saturates in  $H = 5$  kOe. This reliably indicates that the magnetization lies in plane at remanence. In addition, we briefly comment on the magnetization curves ( $M$ - $H$  profiles) recorded in the fields both parallel ( $\theta = 0^\circ$ ) and perpendicular ( $\theta = 90^\circ$ ) to  $\mathbf{k}$  [8]. The remanent magnetizations in both configurations coincide with each other, hence the remanent magnetization is a factor of  $0.7$  smaller than the saturation magnetization. This also supports the fact that the magnetization aligns along the lithographically defined wire axes in each segment for both configurations. Moreover, the magnetization curve in the field parallel to  $\mathbf{k}$  shows a squarelike profile, whereas that in the field perpendicular to  $\mathbf{k}$  exhibits a two-step-like magnetization process. Thus the MR curves and magnetization data can be consistently explained on the basis of the anisotropic magnetoresistance due to the rotation of the magnetization in the film plane.

Next, we show the resistivities in  $H = 0$  as a function of the field orientation  $\theta$  (Fig. 5). Note that two different resistivities are plotted between  $\theta = 40^\circ$  and  $50^\circ$  due to the presence of the hysteresis. A clear discontinuity of the resistivity at about  $\theta = 45^\circ$  is observed in comparison with nearly constant values, respectively, at  $\theta = 0^\circ$ - $40^\circ$  and  $50^\circ$ - $90^\circ$ , which is the clear indication of the negative MR due to the DW accompanied with the change in the domain structure from the single domain to the multidomain at  $\theta = 45^\circ$ . It should be noted that the

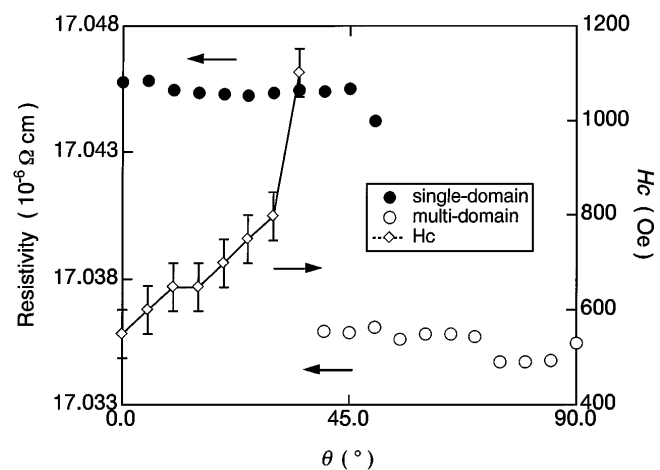


FIG. 5. Field orientation dependence of the resistivities in remanence and the switching fields.

difference in the resistivities between the single domain and the multidomain persists even at 200 K. The negative contribution due to the DW is deduced to be  $-1.8 \times 10^{-6} \Omega \text{ cm}$  on the assumption of a typical DW thickness of 15 nm [4].

We should mention about a few models for the negative MR due to the DWs. The most simple source is the AMR in the DWs [9]. We estimate the AMR contribution of  $-0.25 \times 10^{-6} \Omega \text{ cm}$  using the MR ratio of 1.4% obtained for the single straight Co wire, which is smaller by an order of magnitude than the observed negative resistivity contribution. Recently, the theoretical calculation has predicted the negative MR associated with a domain wall at low temperatures on the basis of the linear response theory. This calculation implies that the wall suppresses the quantum interference between the electrons and decreases the resistivity in the weakly localized regime [5]. Nevertheless, the quantum dephasing effect of the electrons qualitatively disagrees with our results since the negative MR is distinctively observed even at 200 K. A small motion of a DW can also result in the conductance fluctuation (CF) which is suggestively one of the sources of the negative MR in Ni wires [5,10,11]. As we have stated before, we concentrate on the difference of the resistivity only in remanence, i.e., a static DW, in contrast to the results obtained in a sweeping field [1,2]. Thus the CF should be eliminated from the sources in the present case.

In conclusion, we have proposed a novel approach to systematically control the domain structure using the zigzag geometry. This technique has the advantage of tailoring the ferromagnetic submicron wires with a desired domain density. We have also showed clear evidence for the negative magnetoresistance due to the DWs. The decrease in the resistivity due to the domain wall is deduced to be  $-1.8 \times 10^{-6} \Omega \text{ cm}$ , which cannot be explained within the existing theories such as the AMR

effect and the quantum decoherence of the electrons. We further encourage theoretical research to elucidate the origin of the negative magnetoresistance.

The authors thank Professor Eiji Kita, Dr. H. Yanagihara, Dr. T. Furubayashi, and H. Mamiya for helpful discussions and encouragement of this study.

- 
- [1] K. Hong and N. Giordano, *J. Magn. Magn. Mater.* **151**, 396 (1995).
  - [2] Y. Otani *et al.*, in *Proceedings of the MRS Spring Meetings, San Francisco, 1997* (MRS, Warrendale, 1997); Y. Otani, S.G. Kim, K. Fukamichi, O. Kitakami, and Y. Shimada, *IEEE Trans. Magn.* **34**, 1096 (1998).
  - [3] U. Ruediger, J. Yu, S. Zhang, A.D. Kent, and S.S.P. Parkin, *Phys. Rev. Lett.* **80**, 5639 (1998); A.D. Kent, U. Ruediger, J. Y. Zhang, P. M. Levy, and S. S. P. Parkin, *IEEE Trans. Magn.* **34**, 900 (1998); U. Ruediger, J. Yu, S. Zhang, A. D. Kent, and S. S. P. Parkin, *Appl. Phys. Lett.* **73**, 1298 (1998).
  - [4] J.F. Gregg, W. Allen, K. Ounadjela, M. Viret, M. Hehn, S.M. Thompson, and J.M.D. Coey, *Phys. Rev. Lett.* **77**, 1580 (1996).
  - [5] G. Tatara and H. Fukuyama, *Phys. Rev. Lett.* **78**, 3773 (1997).
  - [6] P.M. Levy and S. Zhang, *Phys. Rev. Lett.* **79**, 5110 (1997).
  - [7] I.A. Champbell and A. Fert, in *Ferromagnetic Materials*, edited by E.P. Wohlfarth (North-Holland, Amsterdam, 1982), Vol. 3; T.R. McGuire and R.I. Potter, *IEEE Trans. Magn.* **11**, 1018 (1975).
  - [8] T. Taniyama and I. Nakatani (to be published).
  - [9] L. Berger, *J. Appl. Phys.* **69**, 1550 (1991).
  - [10] P.A. Lee and A.D. Stone, *Phys. Rev. Lett.* **55**, 1622 (1985); P.A. Lee, A.D. Stone, and H. Fukuyama, *Phys. Rev. B* **35**, 1039 (1987).
  - [11] B.L. Al'tshuler, *JETP Lett.* **41**, 648 (1985).